Spatially resolved fast ion velocity distribution results from on-axis and off-axis NBI heated plasmas on ASDEX Upgrade using the Collective Thomson Scattering (CTS)

F. Meo[1], M. Salewski[1], H. Bindslev[1], J. Hobirk[2], S. B. Korsholm[1], F. Leuterer[2], F. Leipold[1], P. K. Michelsen[1], D. Moseev[1], M. Garcıa-Munoz[3], S. K. Nielsen[1], M. Stejner[1], J. Stober[2], G. Tardini[2], D. Wagner[2], and the ASDEX Upgrade team.

[1] *Association EURATOM-Risø National Laboratory for Sustainable Energy, Technical University of Denmark, P.O. Box 49, DK-4000 Roskilde, Denmark*
[2]*Max-Planck-Institut für Plasmaphysik, EURATOM Association, D-85748 Garching, Germany*

Introduction:

Collective Thomson scattering (CTS) experiments have been carried out on ASDEX Upgrade (AUG) to study the effect on the fast ion velocity distribution at different NBI current drive (NBCD) configurations such as on-axis and off-axis injection. Off-axis NBCD is planned to be a key constituent of advanced tokamak scenarios to control the current density profile where off-axis current drive flattens the q-profile leading to enhanced confinement regimes. The motivation of this study comes from past off-axis NBCD experiments that have unveiled deviations from the classical picture under certain operating regimes even in the absence of MHD instabilities [1-3] that can redistribute the fast ions. The CTS diagnostic has the capability to measure the fast ion distribution in magnetically confined plasmas from collective fluctuations along the fluctuation wave vector $\mathbf{k}^{\delta} = \mathbf{k}^{s} - \mathbf{k}^{i}$ where $\mathbf{k}^{s}$ and $\mathbf{k}^{i}$ are the wave vectors of the received scattered radiation and the incident probing beam, respectively. The inferred 1D velocity distribution function *g(u)* is the projection of the 2D ion velocity distribution $f(v_{//}, v_{\perp})$ onto $\mathbf{k}^{\delta}$. The microwave based backscattering CTS system on AUG [4] uses a high power gyrotron as the probe at 105 GHz. The AUG ECRH steerable antenna system enables localized measurement of the confined fast ion distribution at different spatial locations and at different angles of $\mathbf{k}^{\delta}$ to the magnetic field ($\angle(\mathbf{k}^{\delta}, \mathbf{B})$) hence capable of attaining information on the anisotropy. Fast ion measurements at the centre of the plasma under different NBCD configurations are presented below. In addition, direct comparison of the *g(u)* between CTS measurements to the widely used transport code TRANSP [5] coupled with the Monte Carlo neutral beam module NUBEAM [6] has shed some light on the mechanisms that govern the fast ion transport.

The experimental setup and results

The CTS measurements were carried out in low triangularity standard ELMy H-mode plasmas at B_t = 2.6 T and Ip = 800 kA where the central electron density was kept at $n_e(0) = 6 \times 10^{19}$ m^{-3} in feedback mode. AUG is equipped with an NBI system capable of up to 20 MW of power (in deuterium) consisting of two injectors each equipped with four ion sources. The different ion sources have different injection energies ($E_{inj}(D^0)$ = 60 keV and 93 keV) and geometries including on/off-axis injection capability [7]. The CTS scattering geometry used in these experiments is shown in Figure 1. The scattering volume lies at the centre of the plasma and $\angle(\mathbf{k}^\delta, \mathbf{B}) \approx 120°$ where the plasma current **Ip** and direction of the magnetic field **B** are anti-parallel. Figure 2(a) shows the frequency up-shift in the spectral power density due to the $\mathbf{k}^\delta$ being oriented in the same toroidal direction as **Ip** (fast ion flow direction), as expected from $\omega^\delta \approx v_{ion} \cdot k^\delta$. In order to distinguish between ECE radiation and scattering, the probe source (gyrotron) is on/off modulated with 2ms on times. The data contained in Figure 2(a) is an average of a series of gyro pulses during a steady state heating phase. To attain the fast ion distribution function in Figure 2(b), the measured CTS spectra in Figure 2(a) are fitted using a least squares fitting procedure which takes prior information about parameters, including those from other diagnostics, and implements a Bayesian method of inference using a forward scattering model. The error bars in Figure 2(b) represent one standard deviation and includes the uncertainties of parameters from diagnostics other than CTS such as electron/ion temperature, and electron density. More details of the procedure can be found in reference [8] with its application to AUG in reference [9]. The graph in figure 2(b) clearly shows significant effect of the off-axis NBI beam source on the central *g(u)*. In order to reduce beta dependant effects, comparison of the central *g(u)* between two discharges each with on-axis and off-axis beam sources for the same total heating power is illustrated in Figure 3. The measurements are averaged over a series of 2 ms probing radiation pulses during a steady state phase. Both discharges are MHD quiescent according to magnetic and soft X-ray measurements during the two-beam phase. Both discharges have the same density but the central electron temperature for the on-axis case is about 20% higher i.e. Te(0) = 2.3 and 2.8 keV for off-axis and on-axis, respectively. The solid lines in figure 3 are results from TRANSP/NUBEAM simulations.

Discussion

The results show that the difference between both on-axis and off-axis NBCD scenarios are marginal and within the diagnostic's error bars. In addition, the measurements and simulations in Figure 3 show a much better agreement for the NBCD on-axis case. The results suggest an enhanced fast ion diffusion for the off-axis heating configuration. One asset of the CTS is the ability to attain the resolved velocity distribution shape where Reference 9 demonstrates differences in amplitude and shapes of the fast ion distribution between different on-axis NBI heating configurations. However in this comparison, within the error bars, the results do not show strong evidence of energy dependent transport. It is important to note that due to stray radiation inherent in CTS on AUG, the electron cyclotron (ECE) diagnostic was not operational during the experiments. Therefore, more sensitive local measurements of possible core MHD localized events were not possible. Future experiments will include NBI power scan, triangularity scan, and installation of notch filters to render the ECE compatible to CTS. The data presented here is still preliminary and improvements to the fitting procedure is in progress.

List of Figures

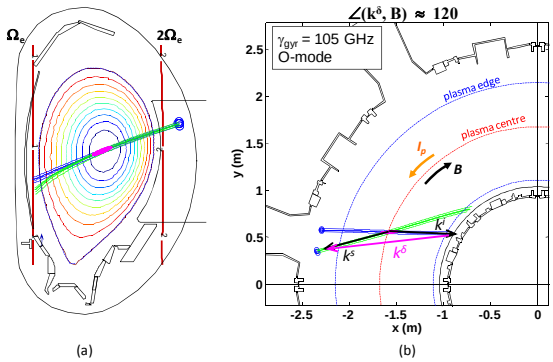

Figure 1. Poloidal view (a) and top view (b) of an example of a scattering geometry of the CTS on ASDEX Upgrade for $\angle(k^{\delta}, B) \approx 120°$. The blue and green traces illustrate the probe and receiver beam respectively. The scattering volume, where the beams overlap, is shown in magenta at the plasma centre.

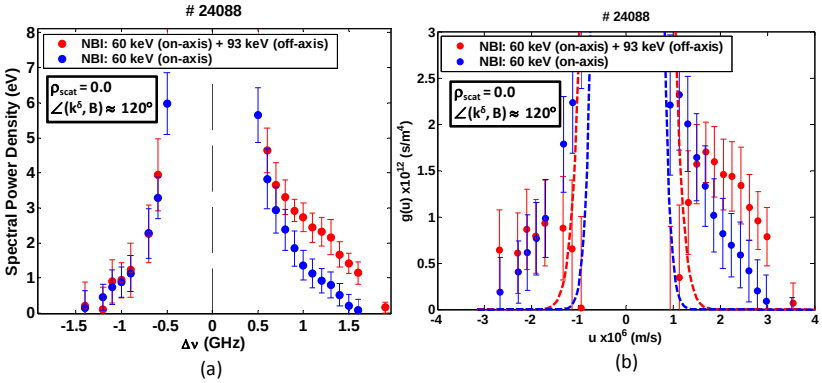

Figure 2. The CTS results that shows the effect of the off axis NBI beam; the red (blue) data points on both graphs represents NBI heating configuration with two (one) ion sources. (a) Spectral power density and (b) fast ion distribution function. The abscissa in (a) is the frequency and in (b) is the velocity component which is along $\mathbf{k}^{\delta}$.

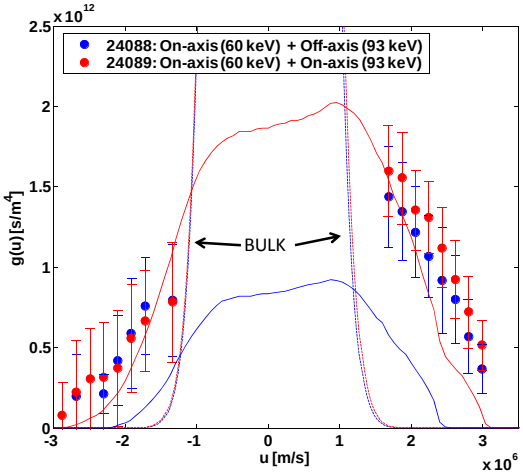

Figure 3. The CTS results of g(u). The dotted lines are the bulk ion distributions. Both discharges have a central source beam with injection energy of 60 keV for D^0. The red (blue) data points represents an additional NBI source with injection energy 93 keV for D^0 with an on-axis (off-axis) configuration. The abscissa is the velocity component which is along $\mathbf{k}^{\delta}$. The solid lines are results from TRANSP/NUBEAM simulations without additional fast particle diffusion

References

1. Hobirk J. et al 2003, 30th EPS Conf. (St Petersburg, Russia) O-4.1B
2. Park J. M. et al Phys. of Plasmas **16**, 092508 (2009)
3. M. Murakami, Nucl. Fusion **49**, 065031 (2009)
4. F. Meo *et al*, Rev. Sci. Instrum., **79**, 10E501 (2008)
5. Budny R.V. et al (1995) Nucl. Fusion 35 1497
6. Pankin A., McCune D., Andre R. and Kritz A. 2004 Comput. Phys. Commun. 159 157–84
7. A. STAEBLER et al., Proc. 18th Symp. Fusion Technology, Karlsruhe, Germany, 1994, p. 593 (1995)
8. Bindslev H et al Rev. Sci. Instrum. 70 1093–1099, (1999)
9. Salewski M et al, Nucl. Fusion 50 035012 (2010)